

Engineered 3D Matrices with Spatiotemporally Tunable Properties

KOICHIRO UTO,^a RIHO TANIMOTO^{a,b} AND
COLE A. DEFOREST^{*c,d,e,f,g}

^a Research Center for Functional Materials, National Institute for Materials Science (NIMS), 1-1 Namiki, Tsukuba, Ibaraki 3050044, Japan; ^b Graduate School of Pure and Applied Sciences, University of Tsukuba, 1-1-1 Tennodai, Tsukuba, Ibaraki 3058577, Japan; ^c Department of Bioengineering, University of Washington, Seattle, Washington 98105, USA; ^d Department of Chemical Engineering, University of Washington, Seattle, Washington 98195, USA; ^e Institute for Stem Cell & Regenerative Medicine, University of Washington, Seattle, Washington 98109, USA; ^f Molecular Engineering & Science Institute, University of Washington, Seattle, Washington 98195, USA; ^g Department of Chemistry, University of Washington, Seattle, Washington 98105, USA
*Email: profcole@uw.edu

13.1 Introduction

It has become widely appreciated that mechanical forces are ever present between cells and their surroundings and that these forces provide a crucial set of cellular signals that can control cell function and fate. In fact, cells sense their surrounding microenvironment mechanically through push/pull-type interactions and exhibit specific biological functions

(e.g. proliferation, differentiation) in response to these forces through a process well known as mechanotransduction.¹ Mechanobiology is the study of how cells perceive surrounding forces presented by the extracellular matrix (ECM) and how they are converted into intracellular biochemical signaling cascades to alter cellular function and fate. To date, our collective insights into cellular mechanobiology processes have been primarily obtained from experiments performed on flat culture substrates with non-physiological mechanics (e.g. polystyrene, glass). Since Engler *et al.* reported in 2006 that the differentiation of human mesenchymal stem cells (hMSCs) strongly depends on the elastic modulus of the substrate using polyacrylamide hydrogels with elastic modulus mimicking biological tissues,² significant efforts have sought to elucidate the relationship between matrix mechanics and cell behavior. However, *in vivo*, cells are embedded in a complex and information-overloaded environment consisting of multiple ECM components and cell types. Biochemical and biophysical signals displayed by and within the ECMs are also presented with spatiotemporal variations. Though static 2D culture platforms have proven useful for understanding cellular phenomena to some degree, these approaches are intrinsically limited in their ability to fully recapitulate the full 4D complexity of signaling cells experience *in vivo*. Thus there is a growing interest in the development of material systems enabling the 3D cell culture with dynamic properties, where changes in physical and biochemical properties of materials can be modulated in a user-defined and/or cell-dictated manner. In this chapter, we focus our attention on the development of 4D-programmable culture matrices that are actively catapulting mechanobiology into a new dimension. Specifically, we will discuss the importance of 3D biomaterials in studying cell function, what can be controlled in spatiotemporal fashion by proposed 4D culture systems, and what physiological phenomena can be recapitulated and explored from the perspective of materials science and mechanobiology.

13.2 The Importance of 3D Cell Culture

Cells are mechanically coupled with their extracellular environments; the cellular niche plays a crucial role in communicating between cell and ECM, as well as mediating cellular responses to various cues. Along with the biochemical and mechanical properties of the ECM, several studies have demonstrated the impact of the culture dimensionality on cell-ECM interactions for regulation of cellular behaviors. This comes as little surprise, given that cells are most often embedded within a 3D matrix *in vivo* that is markedly different from a 2D substrate with respect to cue presentation.³ As a result of the difference in culture dimension (2D *versus* 3D, as shown in Figure 13.1A), cells behave quite differently in their adhesion and biological response. For example, when 3T3 fibroblasts are cultured on collagen-treated glass, the cells take on a spread morphology, develop actin stress fibers, and proliferate more rapidly.⁴ Curiously, 3T3

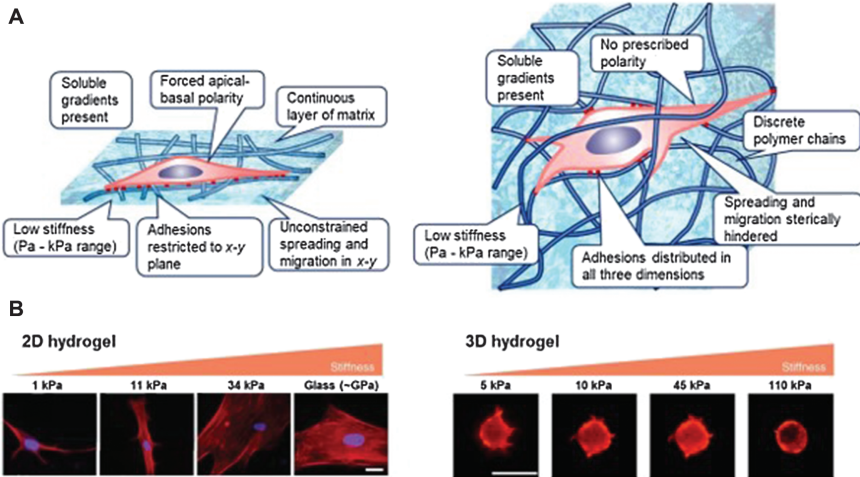


Figure 13.1 Microenvironmental effects on cell function in 2D and 3D culture. (A) Cells experience starkly different cues when cultured on and within materials. (B) Cell morphology depends on culture substrate in 2D but not in 3D. Mesenchymal stem cells cultured on increasingly stiff 2D hydrogel substrate increasing their spread area. Adapted from ref. 5 with permission from Springer Nature, Copyright 2016, while cells encapsulated in 3D hydrogel maintain a round morphology. Adapted from ref. 6 with permission from Springer Nature, Copyright 2010.

fibroblasts exhibit opposite behavior when cultured within a 3D collagen gel; though cell-substrate interactions are promoted through the same integrin-collagen binding, the dimension of culture ultimately defines how these interactions manifest. As previously noted, these cellular behaviors can be further influenced by matrix mechanics, though such mechanobiological responses also vary greatly with culture dimension. Similar seemingly paradoxical behavioral findings have been observed for mesenchymal stem cells (MSCs), where the cells cultured on increasingly stiff 2D hydrogel substrates show increasing spreading⁵ that is unobserved in 3D culture (Figure 13.1B).⁶ Furthermore, mechanosensitive Yes-associated protein (YAP) localization to the nucleus, morphological spreading, and level of stress fiber formation are good predictors of MSC lineage commitment, including both osteogenic and adipogenic differentiation, in 2D culture. In 3D culture, however, all of these variables do not have the same predictive power of MSC fate, highlighting that 3D mechanobiology studies remain largely underexplored.⁷ The mechanism governing such cellular response regulation stems from many interrelated factors, including how the ECM transmits force to the cell and how the ECM/cell are mechanically/biochemically coupled. To better understand these complex mechanobiological phenomena, development of appropriately optimized 3D biomaterials for cell culture remains critical.

13.3 Design Strategy of Engineered Matrices for 3D Cell Culture

When designing engineered matrices for 3D cell culture, one must carefully consider several important aspects, including biomaterial mechanics, biochemistry, biodegradability, and overall biocompatibility.^{8,9} Hydrogels are water-swollen 3D polymeric networks; mimicking various biochemical and tissue-relevant mechanical properties, they have proven to be excellent materials for supporting 3D cell growth. From a biocompatibility perspective, the synthetic polymers such as poly(ethylene glycol) (PEG) and naturally derived polymers (*e.g.* polysaccharides including hyaluronic acid and alginate, collagen, gelatin) have been widely employed. As such gels present average mesh sizes that are typically orders of magnitude smaller than the size scale of eukaryotic cells ($\sim 10\text{--}20\ \mu\text{m}$ diameter), it is often challenging to postsynthetically introduce cells into preformed hydrogels. Hence, direct encapsulation strategies must be developed that enable hydrogels to be created from biocompatible polymers using cytocompatible chemistries in the presence of living cells. Though hydrogels have been synthesized using a variety of chemistries spanning a wide range of reaction conditions, biomaterial formation should avoid those that could cause excessive damage to the cells through excessive free-radical generation, high and large temperature/pH changes, or toxic biproduct formation. Careful consideration of the chemistries must be given to those employed in forming cell-laden hydrogels from biocompatible polymers. To date, several cyto- and biocompatible chemistries have been developed for cell encapsulation within the hydrogels in high viability or intact state (Figure 13.2).

Free-radical chain polymerization is initiated through thermal, photochemical, or oxidative/reductive initiator decomposition into active radicals that can form and crosslink functionalized polymers into 3D networks (Figure 13.2). These chemistries most typically utilize multifunctional acrylates or methacrylates (*e.g.* PEG-dimethacrylate). Though these chemistries are rapid and robust, consideration must be given to the effects of such free radicals, known to transfer nonspecifically onto bioactive substances including proteins and cells, on bioactivity and viability.¹⁰ Under some conditions, such exothermic chemistries may induce localized heating that can damage cells during polymerization.¹¹ Despite these potential problems, several cytocompatible formulations have been devised that have enabled radical chain polymerization to be successfully utilized for cell encapsulation in gels. Bryant and Anseth have shown the encapsulation of chondrocytes into PEG hydrogels by photoinduced free radical polymerization using methacrylated PEG macromers (PEGDM) and water-soluble photoinitiator Irgacure 2959. The viability of the chondrocytes was maintained during the polymerization of hydrogel at lower macromer concentration ($<30\%$), suggesting the biocompatibility of the crosslinking method.^{12,13}

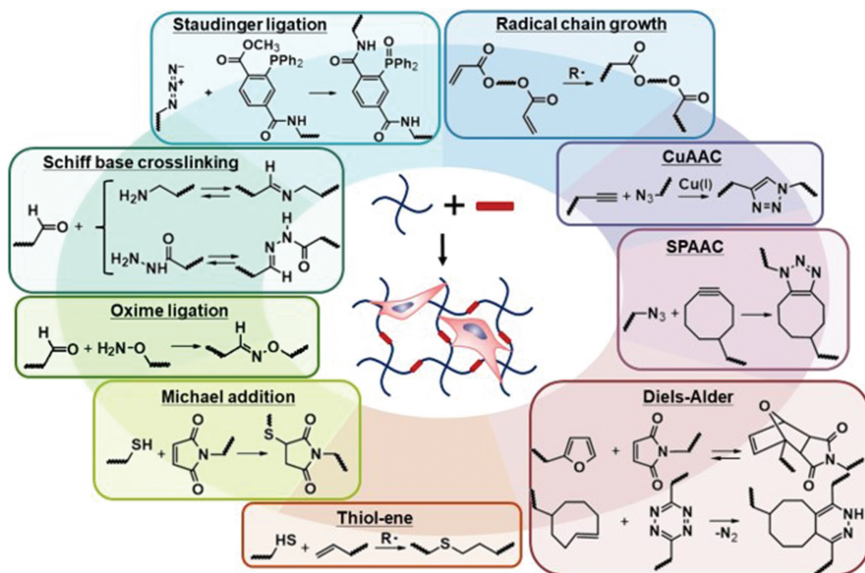


Figure 13.2 Chemistries used previously for efficient encapsulation of living cells within hydrogels. A variety of bioorthogonal and cell-friendly chemistries can be exploited to form and postsynthetically modify hydrogels for 3D cell culture.

Furthermore, recent studies have demonstrated that light conditions typically employed in free-radical polymerization of hydrogels are fully cyto-compatible, causing no changes to the cellular proteome.¹⁴ Though such chemistries are compatible with live cell encapsulation, free-radical polymerization results in a polydisperse molecular weight distribution of the polymer chains that manifests as a molecularly heterogeneous network with nonuniform mechanics.¹⁵ Therefore, the development of methods to form hydrogels with more homogeneous or well-defined network structures, particularly in the context of mechanobiology, is of great interest for 3D cell culture.

13.3.1 Azide–Alkyne Cycloaddition for Engineered Hydrogel Crosslinking

The ideal mechanism used to crosslink engineered hydrogels would utilize chemistries that do not crossreact or interfere with the biology of the system. The field of bioorthogonal chemistry has emerged to address the need for highly specific and robust reactions in biological contexts, and the advantages of bioorthogonal crosslinking strategies can be exploited in hydrogel design to gently and efficiently encapsulate cells within a variety of gel systems.¹⁶ From this perspective, researchers now regularly exploit bioorthogonal click chemistry for hydrogel formation because of its

simplicity, extremely high reaction selectivity and efficiency, and its ability to be performed in water. The azide-alkyne cycloaddition reaction is the most common bioorthogonal chemistry used for cell encapsulation. The early study for hydrogel formation by azide-alkyne cycloaddition used copper(I) as a catalyst,¹⁷ but the potential cytotoxicity of copper has limited the use of this reaction for cell encapsulation (Figure 13.2). However, several cell types, including human foreskin fibroblasts (HFF-1), human adipose-derived mesenchymal stem cells (hMSCs), and human umbilical vein endothelial cells (HUVECs), have been shown to tolerate copper exposure during the crosslinking process,¹⁸ and it is possible that copper-binding ligands such as tris(hydroxypropyltriazolyl)methylamine (THPTA), which is known to reduce cytotoxicity, can be used in crosslinking for other cells.¹⁹ To overcome this problem of copper cytotoxicity, DeForest *et al.* utilized a copper-free click chemistry based on strain-promoted azide-alkyne cycloaddition (SPAAC) reaction between azide and difluorinated cyclooctyne (DIFO) groups developed by Bertozzi *et al.*^{20,21} to produce biocompatible PEG hydrogels for cell encapsulation (Figure 13.2).²² In this early example, spontaneous hydrogel formation was preceded by crosslinking azide-functionalized 4-arm PEG (4-arm PEG-N₃) with a bisDIFO-functionalized peptide that could be enzymatically cleaved by cell-secreted matrix metalloproteases (MMPs). Using this approach, NIH3T3 fibroblasts were encapsulated with PEG hydrogels through SPAAC, and they demonstrated high viability after 24 hours with the biomaterial. Subsequently, the group also demonstrated that the mechanical properties of such hydrogels can be tuned by changing the molecular weight of the 4-arm PEG-N₃ and the molar ratio of azide and DIFO groups.²³ Early cyclooctyne derivatives such as DIFO had comparatively slow reaction kinetics, requiring several tens of minutes to complete crosslinking by SPAAC reaction, and were challenging to synthesize.²⁴ To improve the kinetics for bioorthogonal crosslinking, dibenzylcyclooctyne (DBCO) derivatives were developed through fusion of two benzyl rings to and inserting an amide-linked nitrogen into the cyclooctyne ring. It has been reported that the reaction rate can be improved by up to one order of magnitude over other SPAAC reactions.²⁵⁻²⁷ Hermann *et al.* reported the rapid encapsulation of rmGremlin, a BMP inhibitor, through *in situ* crosslinking of hydrogels using azide-functionalized PEG and DBCO-functionalized PEG crosslinkers, which was completed within 2 min.²⁸ By using DBCO-based SPAAC, cells such as chondrocytes and MSCs were successively encapsulated within various matrices such as dextran and PEG hydrogels efficiently and with high viability.^{29,30} Furthermore, the use of highly strained bicyclic cyclooctyne (BCN), in which a cyclopropane ring is fused to cyclooctyne, has also led to SPAAC reactions with fast reaction kinetics comparable to that involving DBCO.³¹ BCN has advantages over DBCO in terms of being more accessible synthesis, less hydrophobic, and more optically transparent. DeForest and Tirrell demonstrated SPAAC-crosslinked hydrogels using 4-arm PEG tetraBCN for encapsulation of hMSCs, a platform that was used

to promote spatially controlled osteogenic differentiation in response to photopatterned protein immobilization.³² Madl *et al.* reported the encapsulation of hMSCs, HUVECs, and murine neural progenitor cells (mNPCs) within elastin-like protein (ELP) hydrogels by SPAAC reaction between BCN- and azide-functionalized ELP.³³ By varying the amount of BCN groups per ELP, the mechanical property of SPAAC-crosslinked ELP hydrogels can be tuned; hMSC encapsulation was achieved with remarkably high cell viability (~100%). In terms of bioorthogonal reactions, the potential reactivity of cyclooctynes with free thiol, including those found on cysteine residues, presents some concern, and indeed some cyclooctynes are known to undergo such thiol-yne reactions under physiological conditions.^{25,34} However, since few free thiols exist in the physiological environment and the second-order reaction rate of SPAAC is significantly higher than that of the thiol-yne reaction ($10^{-1} \text{ M}^{-1} \text{ s}^{-1}$ and $10^{-4} \text{ M}^{-1} \text{ s}^{-1}$ for BCN-azide and BCN-thiol reaction, respectively), SPAAC is recognized practically as a true bioorthogonal reaction. In addition to SPAAC reactions, noncatalyzed azide-alkyne cycloaddition reactions in water using terminal alkynes with adjacent electron-withdrawing substituents have also been proposed.³⁵ Truong *et al.* succeeded in rapid gel formation at 37 °C by mixing azide-functionalized chitosan (CS-azide) with propiolic acid ester-functionalized PEG (PEG-alkyne) in the presence of hMSCs, establishing a promising alternative copper-free click chemistry to construct engineered 3D matrices.³⁶

13.3.2 Diels–Alder Reaction for Engineered Hydrogel Crosslinking

The Diels–Alder (DA) reaction is also classified as a click reaction due to its simplicity, high efficiency, and selectivity; the reaction is widely used for hydrogel crosslinking. In general, when DA reaction is used for organic synthesis, high temperatures are required to achieve moderate reaction rates, though a hydrophobic effect accelerates the reaction dramatically when performed in water. Several diene–dienophile reactions have proven useful for bioorthogonal hydrogel crosslinking (Figure 13.2).

Wei *et al.* first reported the preparation of hydrogels by DA reaction using poly(*N,N*-dimethylacrylamide-*co*-furfuryl methacrylate) as the diene and *N*-[4-formyl polyethylene glycol ester] bismaleimide as the dienophile.³⁷ In this system, the DA reaction is accelerated in water, and the gelation time is about 1 h. Nimmo *et al.* also synthesized furan-modified hyaluronic (HA) acid and dimaleimide PEG and reported a facile method to prepare HA hydrogels *via* aqueous-based DA reaction.³⁸ Both the mechanical properties and degradability of HA hydrogels can be tuned by adjusting the molar ratio of furan to maleimide on the HA and PEG. The results of culturing human adenocarcinoma cells (MDA-MB-231) on HA hydrogels showed high viability

(>98%) even after 14 days of culture, indicating that the hydrogels have excellent cytocompatibility.

The furan/maleimide reaction is the most used DA chemistry for hydrogel formation, though it lacks complete bioorthogonality. In addition to their potential to crossreactivity with thiol-containing amino acids such as cysteine and the primary amine found on lysine side chains, maleimides have also been noted to be susceptible to hydrolysis.³⁹ Blackman *et al.* were the first to report that the inverse electron demand Diels–Alder (IED-DA) reaction between dipyrindyl-tetrazine and *trans*-cyclooctene is useful for bioconjugation.⁴⁰ This reaction proceeded rapidly without a catalyst, proceeding up to three orders of magnitude faster than SPAAC. As an alternative, norbornene can be used as the dienophile in place of *trans*-cyclooctene. Zhou *et al.* developed the IED-DA reaction between norbornene and tetrazine for the preparation of PEG hydrogels.⁴¹ Subsequently, Alge *et al.* successfully prepared cell-laden hydrogels using the IED-DA reaction.⁴² Mixing of 4-arm PEG-tetrazine macromer and dinorbornene-modified peptide yielded stable gels within a few minutes by IED-DA and hMSC encapsulation with high viability. In addition to rapid kinetics, the IED-DA reaction is characterized by high bioorthogonality and yields irreversible crosslinking, which differs from the typical DA reaction.

13.3.3 Thiol–Ene Reaction for Engineered Hydrogel Crosslinking

Thiol–ene chemistry involves a reaction between a thiol and an unsaturated alkene (*e.g.* acrylate, maleimide, norbornene) through free-radical or catalyzed Michael addition (Figure 13.2). Unsaturated functional groups may react with thiol and amino groups on biomolecules, which yields incomplete bioorthogonality. Despite this, the reaction is commonly deemed to have “click” status because it occurs rapidly and with high selectivity/yield under mild conditions.⁴³ Rydholm *et al.* have successfully used poly(ethylene glycol)-*b*-poly(lactic acid) (PEG-PLA)-diacrylate and multivalent thiols to form hydrogels by thiol–ene click reaction *via* photoinitiation and mixed step-chain growth reactions.⁴⁴ Furthermore, a photopolymerization reaction using PEG-dimethacrylate and RGDS peptides containing four cysteine residues was successfully used to encapsulate hMSCs within hydrogels with high viability, demonstrating its usefulness for *in situ* crosslinking in the presence of cells.⁴⁵

This thiol–ene click reaction is not limited to the reaction with thiol-acrylate or thiol-methacrylate. Lutolf *et al.* reported a base-catalyzed Michael-type addition reaction between thiol and vinyl sulfone using 4-arm PEG-vinyl sulfone and bis-cysteine-peptide to produce hydrogels under relatively mild conditions (pH of 8.0) that support cell encapsulation.^{46–48} The Michael-type addition reaction does not involve the generation of cytotoxic free radicals or

UV irradiation but does require a nucleophilic buffer such as triethanolamine (TEA) to promote the reaction. Phelps *et al.* formed hydrogels using 4-arm PEG with terminal maleimides and bis-cysteine-containing peptides.⁴⁹ This Michael-type addition between maleimide-thiol showed higher reactivity than that of acrylate-thiol or vinyl sulfone-thiol, permitting rapid PEG hydrogel formation with less TEA. Although TEA is toxic to some cell types (*e.g.* endothelial cells⁵⁰), the Michael-type addition of thiol-maleimide allows C2C12 murine myoblasts encapsulation within hydrogels with high survival. Hydrogels using step-growth polymerization, which occurs in this complementary reaction mechanism, have been shown to form a uniform network structure with superior mechanical properties compared to hydrogels with same crosslinking density obtained through chain-growth polymerization.^{15,51} However, the alkaline conditions required to promote the kinetics of hydrogel formation may promote the formation of disulfide bonds, leading to reduced bioorthogonality and the formation of hydrogels with nonstoichiometric compositions. Fairbanks *et al.* reported PEG hydrogels formed by thiol-norbornene photopolymerization.⁵² The photo-initiation of radicals enables rapid network formation by a step-growth mechanism, demonstrated to be cytocompatible with hMSC encapsulation. In addition, *in situ* crosslinking by the photopolymerized step-growth mechanism not only affords hydrogels with a uniform network structure but also enables temporal and spatial control over formation unattainable using spontaneous Michael-type chemistries.

13.3.4 Other Reactions for Engineered Hydrogel Crosslinking

Carbonyls such as aldehydes and ketones are absent from proteins and DNA, making them useful targets for bioorthogonal reactions. Ligation of carbonyls with primary amines through imine formation is difficult to perform in water or neutral pH conditions due to the poor thermodynamic stability of imines, reaction reversibility, and the need for harsh acidic dehydration condensation conditions. Conversely, oxime ligation occurring between an alkoxyamine/hydroxylamine and a carbonyl has proven useful for hydrogel formation (Figure 13.2). Grover *et al.* demonstrated the preparation of oxime-linked PEG hydrogels by mixing glutaraldehyde with 8-arm PEG containing alkoxyamine as an end group.⁵³ The formation of oxime bonds can be catalyzed by acid, but rapid gelation within 30 minutes was observed even at pH 7.2; murine MSCs were encapsulated within the hydrogel with high viability. Since glutaraldehyde, which was used as a crosslinking agent, can take on a variety of structures depending on pH and may react with primary amines in proteins and cells, optimization of conditions is necessary to achieve bioorthogonality and the click nature of the reaction. Furthermore, the hydrogels with excellent stability can be formed *via* oxime ligation between alkoxyamine and aldehyde due to its essentially irreversible nature at neutral pH, which is different from hydrazone and imine-based reactions (Figure 13.2). Notably, a photomediated oxime ligation exploiting a

photocaged alkoxyamine has been reported that provides spatiotemporal control over gel formation/modification in a radical-free bioorthogonal manner.^{32,54,55}

Staudinger ligation is a reaction that occurs between phosphine and azide, producing aza-ylide (Figure 13.2). In the presence of water, this intermediate undergoes spontaneous hydrolysis to yield a primary amine and the corresponding phosphine oxide. The reaction of phosphine and azide proceeds with high efficiency under aqueous solution conditions at room temperature. Saxon and Bertozzi found that electrophilic traps, such as methyl esters at appropriate positions in the phosphine structure, capture the nucleophilic aza-ylide by intramolecular cyclization, ultimately producing a stable amide bond rather than the hydrolyzed product.⁵⁶ Madl *et al.* designed elastin-like proteins (ELPs) containing the azide and triarylphosphine and prepared ELP hydrogels by Staudinger ligation.³³ Although the gelation rate was about 20 times slower than the SPAAC reaction between BCN and azide moieties, the gelation of ELPs can be achieved within 20 min by adjusting the molar ratio of azide to triarylphosphine. Gattás-Asfura *et al.* also reported the formation of hydrogels and encapsulation of mouse insulinoma (MIN6) cells by Staudinger ligation between azide-modified alginate and 4-arm PEG with triarylphosphines as the end group.⁵⁷ The encapsulated MIN6 cells showed high viability and proliferation in the hydrogel, indicating that the crosslinking of hydrogels using Staudinger ligation is cytocompatible and bioorthogonal.

13.4 Engineered Matrices for 4D Cell Culture

The extracellular microenvironment regulates cell behavior and function through a myriad of spatially and temporally coordinated cues, wherein misrepresented signals can lead to dysfunction and disease. To better understand basic biology and engineer effective strategies for regenerative medicine, researchers must unravel the complex picture of the extracellular microenvironment and develop ways to mimic these functions *in vitro*. This section describes technologies for 4D biology – cell-laden matrices that recapitulate the heterogeneity of tissues and organs both in 3D space and time. In particular, cells *in vivo* are not only embedded within a 3D matrix but also actively remodel this ECM to enable spreading, migration, proliferation, and differentiation. For many applications, it is essential to outfit engineered biomaterials with the ability to undergo dynamic physiochemical alterations similar to those in the native ECM. In this section, we will discuss two distinct types of hydrogel materials that provide a dynamic environment for cells: programmable hydrogels and adaptable hydrogels.

13.4.1 Programmable Hydrogels Based on Degradability

The hydrogel systems introduced in Section 13.3 and most frequently utilized in the biomaterials community are generated through chemical

13.4.1.1 Proteolytically Degradable Hydrogels as Engineered Matrices

Proteolytically degradable hydrogels have been designed that respond to cell-secreted enzymes, allowing for the matrix softening and remodeling on a cell-dictated timescale. This has most frequently been achieved through inclusion of proteolytically sensitive degradable peptide crosslinkers, in which site-specific modifications to the substrate sequence can yield materials with very different degradative profiles.⁴⁶ To examine how the chemical crosslink density and gel affects encapsulated hMSCs' fate, the Burdick group employed RGD-modified methacrylated hyaluronic acid (MeHA) hydrogels.⁵⁸ Chain-growth photocrosslinking enabled hMSC encapsulation, with gels of varying elastic moduli attainable depending on the MeHA macromer concentration. When hMSC-laden hydrogels were cultured in bipotential osteogenic/adipogenic medium, hMSCs in MeHA gels of all elastic moduli (about 4–91 kPa) underwent almost exclusively adipogenic differentiation, implying that matrix mechanics and crosslink density have little effect on stem cell fate in nondegradable hydrogels. In addition, they synthesized methacrylate- and maleimide-modified HA (MeMaHA) and constructed a multistep crosslinkable hydrogel; here, the Michael-type reaction of maleimide-thiol yielded a primary crosslinking reaction for initial gel formation, while the photoinitiated chain-growth reaction of methacrylate groups could be independently triggered for secondary crosslinking. For hMSCs encapsulated within MMP-degradable HA hydrogels (~4 kPa) prepared by Michael-type reaction crosslinking, osteogenic outpaced adipogenic differentiation after 14 days in culture, though the opposite trend was observed when nondegradable secondary crosslinks were introduced immediately after cell encapsulation (Figure 13.3B). Furthermore, experiments using 3D traction force microscopy (TFM) demonstrate that differentiation of hMSCs encapsulated within covalently crosslinked HA hydrogels were induced by the generation of degradation-mediated cellular traction forces, independent of cell morphology and matrix modulus. Thus hMSCs encapsulated in HA hydrogels with comparable elastic moduli have higher (lower) degree of cell spreading and

Figure 13.3 Designing the degradability of 3D hydrogels and its application for manipulating cellular functions: (A) The degradability of chemically crosslinked hydrogels can be manipulated in preprogrammed, cell-dictated, or user-defined manner using different labile groups. Reproduced from ref. 8 with permission from the Royal Society of Chemistry. (B) examples of control of MSC differentiation using proteolytically degradable hydrogels: Adapted from ref. 58 with permission from Springer Nature, Copyright 2013. (C) Hydrolytically degradable hydrogels for organoid formation: Adapted from ref. 65 with permission from Springer Nature, Copyright 2016. (D) Spatiotemporal control of MSC morphology using photolytically degradable hydrogels: Adapted from ref. 71 with permission from AAAS, Copyright 2009.

traction force, which favors osteogenesis (adipogenesis). Interestingly, they revealed that switching the hydrogel from a permissive to a constrained state through staged secondary crosslinking suppressed hydrogel degradation and traction, triggering a shift from osteogenic to adipogenic differentiation while cells remained spread. These results clearly indicate the importance of matrix degradability on crosslinking and cell morphology, differing from 2D culture where elastic modulus dominantly affects hMSC differentiation.

Cell-degradable materials have also proven essential in maintaining organoid function *in vitro*. Organoids are formed through self-assembled stem cells and resemble their native counterparts in cellular composition, multicellular structure, and functional characteristics. Therefore, organoids have attracted much attention as a powerful tool for basic and translational research.^{59,60} Current organoid culture methods are largely based on animal or naturally derived hydrogels (*e.g.* Matrigel, collagen); there is a growing need for the development of synthetic ECM analogs that offer better reproducibility and user-defined properties. Cruz-Acuña *et al.* established a robust and reproducible methodology for designing the chemically well-defined enzymatically degradable PEG hydrogels to promote the expansion and growth of human intestinal organoids (HIOs) *in vitro*.⁶¹ These engineered hydrogels mainly consist of 4-arm PEG with maleimide group at each end, a cysteine-containing RGD peptide (GRGDSPC) as an adhesive ligand, and bis cysteine-protease-sensitive peptide (GCRDGPQG↓IWGQDRCG; ↓ denotes enzymatic cleavage site) as a degradable crosslinker. When components were mixed in HEPES buffer at pH 7.4 in the presence of cells, gel formation occurred spontaneously by Michael-type addition, and HIOs and human lung organoids (HLOs) could be encapsulated. The mechanical properties of the hydrogel can be tuned by changing the polymer concentration, with PEG hydrogels prepared at ~4.0 wt% displaying mechanics comparable to Matrigel ($G' = 78$ Pa, $G'' = 5.8$ Pa) were determined suitable for the long-term viability of encapsulated HIOs. In addition to the network's biochemical/mechanical properties, hydrogel degradability was demonstrated to be critical to the long-term viability of HIOs; HIOs cannot survive extended culture in non-degradable PEG hydrogels prepared with 1,4-dithiothreitol instead of MMP-degradable peptide crosslinkers. This fully synthetic hydrogel enabled the *in vitro* establishment of intestinal organoids from human pluripotent stem cell (hPSC)-derived spheroids and HLOs from human embryonic stem cells (hESCs). Furthermore, the dynamic and specific mechanical environment was reported as crucial in regulating epithelial cell cyst formation, polarization, and lumen formation, while cell-gel adhesivity regulates apicobasal polarity and lumenogenesis, leading to epithelial cell morphogenesis in a 3D culture system.⁶² Finally, the authors demonstrated the improvement of HIO engraftment and colonic wound repair through gel injection within injured intestinal mucosa, highlighting the material's potential utility as an injectable therapy.

13.4.1.2 Hydrolytically Degradable Hydrogels as Engineered Matrices

While proteolytically sensitive materials can be degraded on timescales dictated by cell state, in many applications it is desirable to preprogram material response profiles into gels. Since hydrogels environments are inherently aqueous, this has been most commonly achieved through network hydrolysis. Several hydrolytically hydrogels have been developed in which hydrolyzable moieties are introduced into the backbone or crosslinking agent of the networks; ester units are most commonly included, decomposing into nontoxic carboxylic acids and alcohols. In such hydrolyzable hydrogels, the chemical properties of the network (*e.g.* crystallinity, hydrophobicity), crosslinking density, and local pH affect the degradation rate. Though material degradation can be tuned, hydrolyzable biomaterials have been most frequently designed to exhibit slower degradation kinetics than the enzymatic degradation just described, theoretically matching the rate of gel hydrolysis with that of encapsulated cell ECM production (Figure 13.3A). In an early study, Rice and Anseth utilized PEG-dimethacrylate (PEG-DM) and PLA-*b*-PEG-*b*-PLA-dimethacrylate (PEG-PLA-DM) as macromers to culture chondrocytes in 3D.⁶³ With PEG-based macromers, chondrocyte-laden PEG hydrogels were prepared by inducing chain-growth radical polymerization by UV irradiation at 365 nm. PEG-DM gives a nondegradable PEG hydrogel, whereas the hydrogel prepared from PEG-PLA-DM contains the hydrolytically degradable PLA moiety, enabling gradual increase in gel swelling, and finally solubilization over the period of approximately 10 days.⁶⁴ The mixture of these two PEG macromers can produce PEG copolymer hydrogels that exhibit bimodal degradation profiles in a narrow composition range (PEG-DM/PEG-PLA-DM = 19:81 ~ 25:75 mol%) where the structural integrity of PEG hydrogels is minimally maintained after degradation, while allowing for a uniform spatial distribution of large ECM components. The stable PEG network provides mechanical support to encapsulated chondrocytes and promotes phenotype maintenance. In fact, the mechanical properties of formed tissues obtained by long-term culture were superior to those of PEG-PLA-DM hydrogels, which show fast and monomodal degradation, especially in the early stages of neocartilage development. Additionally, compared to the nondegradable PEG-DM hydrogel, the most rapidly degradable hydrogel yielded enhanced production and a more uniform spatial distribution of chondrocyte-secreted collagen type I. On the other hand, the slower degrading PEG copolymer hydrogels (PEG-DM/PEG-PLA-DM = 23:77 mol%) suppressed differentiation while maintaining moderate cell morphology and type II collagen distribution within the hydrogels. These results highlight the importance of preprogrammed hydrolytic degradation in 3D cell culture, specifically with chondrocytes for cartilage tissue formation.

Hydrolyzable hydrogels, whose degradation rate can be macroscopically tuned at the molecular level, can be applied to create intestinal organoids

with a higher level of multicellular structure. Gjorevski *et al.* reported that intestinal stem cell (ISC) expansion, differentiation, and interstitial organoid formation were enhanced within hydrolytically degradable hydrogels (Figure 13.3C).⁶⁵ ISCs were encapsulated within PEG hydrogels enzymatically formed through thrombin-activated transglutaminase factor XIII (FXIIIa)-mediated ligation of 8-arm PEG modified with FXIIIa substrate peptides. Though stiffer hydrogels (shear modulus of about 1.3 kPa) supported more cell proliferation than softer ones (shear modulus of 0.2 kPa), stiff gel did not support cell differentiation or organoid formation. To achieve spheroid growth and morphogenesis, the hydrogels needed to be softened from 1.3 kPa to about 0.2 kPa after cell expansion. To do so, the Lutolf group introduced TG-FXIII substrate peptides into vinylsulfone-functionalized 8-arm PEG and acrylate-functionalized 8-arm PEG by Michael-type reaction and crosslinked them by adding thrombin-activated FXIIIa to form chemically stable hydrogels (sPEG) and hydrolyzable hydrogels (dPEG), respectively. Hybrid PEG hydrogels that gradually degrade and soften were prepared through copolymerization, with the profile of degradation and softening controlled by changing the ratio of sPEG to dPEG during the network formation. In addition, enzymatically crosslinked PEG hydrogels modified with RGD peptides derived from FN (fibronectin) and one from LMN (laminin) supported the growth but not differentiation of mouse intestinal organoids. With laminin-111 and enzymatically crosslinked hybrid PEG gels, they succeeded in creating a mechanically dynamic 3D matrix that has the high elastic modulus required for YAP activation and ISC expansion but then softens to relax the accumulation of compressive forces exerted by cells, allowing for *in vitro* organogenesis. Here, the dynamic changes in bulk mechanical property of the hydrogel would also be modulated by processes that simultaneously affect other environmental properties, such as ligand accessibility, clustering, and nanomechanical responses to cell-exerted forces after ligand binding.^{66–69} The intestinal organoid, or “Mini-gut”, produced using such designer materials is expected to have a wide range of applications not only in stem cell research but also in pathological models such as colorectal cancer and cystic fibrosis and regenerative medicine.⁵⁹ These results highlight the importance of hydrolytic degradability for 3D cell culture.

13.4.1.3 Photolytically Degradable Hydrogels as Engineered Matrices

As an alternative to enzymatic or hydrolytic degradable hydrogel systems, light can be used to induce the degradation of hydrogels and the associated changes in mechanical properties. Although degradation is induced in the presence of cells, as in enzymatic and hydrolytic degradation, light can be used to achieve user-defined temporal and spatial control in a highly controlled manner.⁷⁰ The Anseth group first demonstrated that 3D cell-material interactions could be dynamically and externally directed by

photodegradable hydrogels.^{71–73} Acrylated *ortho*-nitrobenzyl (*o*NB) ester-derived moieties (PDA) that can be radically polymerized but photolytically cleaved are appended onto the end of linear PEG molecules (yielding PEG-diPDA); the resulting gel mechanics can be tuned precisely with high spatiotemporal precision using light. Kloxin *et al.* prepared cell-laden photodegradable PEG hydrogels by mixing PEG-diPDA, PEG-monoacrylate (PEGA), fibronectin, hMSC, and free-radical redox initiators in phosphate-buffered saline.⁷¹ Gel photolysis can be tuned by the wavelength (365 nm or 405 nm) and irradiation intensity. When light irradiation is ceased, photodegradation halts, and the mechanical properties are stably maintained; staged light exposures yield stepwise softening of the hydrogel. By changing gel mechanics through network photodegradation, the morphology of encapsulated hMSCs was dynamically regulated; photochemically softened gels yielded higher cell spreading than those maintained at high stiffness (Figure 13.3D). Functionalized PEG macromers modified with variably substituted *o*NB groups have also been utilized to tune PEG gel photodegradation rates and wavelength responsiveness; degradation rate was increased by decreasing the number of aryl ethers on the *o*NB group or changing the functionality from primary to secondary at the benzylic site.⁷⁴ Encapsulation of hMSCs with high viability (~90%) was achieved by redox-initiated free radical polymerization between PEG-acrylate (PEGA) and the developed PEG-diPDA, and wavelength-biased release of encapsulated cells was achieved using bilayer PEG hydrogels crosslinked with two different degradable PEG-diPDA. These results showed that the operability of user-defined photolysis can be extended by material design.

Many of the photodegradable groups used in 3D culture systems, including those based on *o*NB, yield one-photon/one-event responsiveness. In this case, the photodegradable groups incorporated into the hydrogel absorb photons and undergo cleavage reactions, which require large light dosages or high quantum yields for rapid degradation. As many of the photodegradable groups are UV responsive and prolonged or intense irradiation may cause phototoxicity, there has been interest in constructing systems that exhibit more efficient degradation. To achieve this, Brown *et al.* reported on the amplification mechanism of photolysis *via* addition-fragmentation chain transfer (AFCT) reaction.⁷⁵ They focused on the use of allyl sulfides as efficient AFCT functionalities⁷⁶ and synthesized a new azide crosslinker containing allyl sulfide (PEG3-azide). A PEG hydrogel was prepared by SPAAC reaction of PEG3-azide with cyclooctyne-terminated 4-arm PEG (4-arm PEG-DBCO). The PEG hydrogel was cleaved by light irradiation in the presence of photoinitiator and monofunctional thiol, whereby the hydrogel reverted to a soluble branched macromer. In this process, photogenerated thiyl radicals propagate rapidly through thiol–ene addition reactions and chain transfer events. The thiyl–thiol chain transfer events allowed for the cleavage of multiple crosslinking points with a single absorbed photon, and the change of storage modulus (G') of the hydrogel upon photodegradation could be tuned based on the amount of free monofunctional thiol (PEG-SH) added.

This hydrogel degradation *via* the AFCT reaction was strongly influenced by the kinetics of the allyl sulfide exchange depending on the thiol's pK_a ; the acetamide-type allyl sulfide (AS-AA, $pK_a = 10.4$) crosslinker, with a higher pK_a , exhibited faster degradation than propionamide types (AS-PA, $pK_a = 8.8$) and phenyl acetamide (As-PhAA, $pK_a = 6.6$). Based on this fact, they constructed a cell-friendly degradation system for PEG hydrogels using glutathione (GSH, $pK_a = 9.42$) as a free monofunctional thiol. In the presence of a low concentration of soluble thiol (GSH at 15×10^{-3} M) and photoinitiator [lithium phenyl-2,4,6-trimethylbenzoylphosphinate (LAP) at 1×10^{-3} M], the PEG hydrogel was completely degraded within 15 s by irradiation with 365 nm light [5 mW cm^{-2}]. Colony formation from single ISCs encapsulated within this PEG hydrogel was mechanosensitive, and the highest efficiency was achieved with RGD-functionalized hydrogels with moderate storage modulus of approximately 1.5 kPa. The rapid degradation of the PEG hydrogel also allowed the isolation of encapsulated ISC colonies, and colony formation was confirmed again when the colonies were reseeded within the allyl sulfide PEG hydrogel after isolation. This indicates that the allyl sulfide PEG hydrogel is useful for the growth and amplification of ISCs. This AFCT reaction-based degradation is potentially useful for particularly sensitive cell types since it significantly reduces the concentration of photoinitiating species and exposure to light and radicals and can be applied to the degradation of thicker hydrogels (scaffolds).

13.4.2 Engineered 3D Matrices with Spatiotemporally Programmable Biochemical Cues

In degradable hydrogels, the dynamic mechanical environment of surrounding cells can be created as the material degrades in preprogrammed, cell-dictated, and/or user-defined manners. Complementing these mechanical signals in regulating the function of cells and tissue *in vivo* are biochemical cues, whereby cues are presented and interact in complex and synergistic manners. In 2D culture systems, a dynamic interface (see Chapter 6) has been realized to enable switching of various biochemical factors. The ability to spatiotemporally modulate the presentation of proteins, peptides, and small molecules within 3D biomaterials represents an important step toward capturing the dynamic heterogeneity of native tissue.

The Anseth group demonstrated that 3D cell-material interactions could be dynamically and externally directed where peptides are photochemically released from gels with light.⁷¹ They successfully demonstrated the ability to pattern the hydrogels in both 2D and 3D using masked flood irradiation and two-photon laser scanning microscopy, respectively. Using this photo-releasable strategy, Kloxin *et al.* established that the time-dependent presentation of the integrin-specific ligand RGDS significantly enhanced the differentiation of hMSCs into chondrocytes compared to hMSCs cultured with persistent RGDS signaling, suggesting the importance of temporal cue presentation. In their system, both biochemical and biophysical cues within

the PEG hydrogel platform could be dynamically manipulated with photoirradiation, although these cues were only tuned independently of one another in this study. In a follow-up study, DeForest and Anseth successfully created a 3D system that allowed for independent spatiotemporal regulation of biochemical and biophysical cues that influence 3D cell migration.^{22,73} They designed PEG hydrogels *via* SPAAC reaction between difluorinated cyclooctyne-functionalized 4-arm PEG (4-arm PEG-DIFO) and bisazide-functionalized peptides that allow for the photocleavage of crosslinks (biophysical cue) and photoconjugation of pendant functionalities (biochemical cue). With visible light irradiation with eosin Y as photoinitiator, thiol-containing biomolecules (*e.g.* RGD peptide) could be covalently bonded to vinyl functionalities in the hydrogel using thiol-ene reactions (Figure 13.4A). In the presence of UV light, however, *o*NB moieties embedded within the peptide crosslinker are cleaved to yield network photodegradation. Both photocleavage and photoconjugation reactions could be used orthogonally in a wavelength-dependent manner to independently regulate the biophysical and biochemical properties of the hydrogels. This system was exploited for real-time manipulation of cell function, including guiding 3T3 fibroblast migration and outgrowth behavior within peptide-functionalized microvascular channels (Figure 13.4B). Here, patterned control over RGD biochemical presentation and network biophysics proved essential for directing 3D fibroblast migration within the PEG hydrogel. Importantly, these studies also illustrate the ability of such wavelength-dependent chemistries to spatiotemporally define microenvironmental niches that could potentially recapitulate those found *in vivo*. Collectively, these studies are representative of the emerging field of 4D cellular biology, and other promising approaches have been utilized to control various cellular functions in a dynamic and spatially defined manner.⁷⁷⁻⁷⁹

Though the aforementioned photochemical strategies have enabled patterned immobilization of biochemical cues within synthetic gels, these systems lack the capability to reversibly present biochemical cues in a dynamic manner akin to that in native tissue. DeForest and Anseth first demonstrated that the combination of two orthogonal, biocompatible photoreactions based on the combination of the two shown in Figure 13.4C enables the reversible spatial presentation of biological peptide cues.⁸⁰ Peptides (*e.g.* RGD) were synthesized to contain both a thiol group for visible light-mediated photocoupling and an *o*NB moiety for UV-induced photocleavage; utilizing differently colored lights allowed peptides to be first attached and subsequently removed from PEG hydrogels on demand and with 4D control. They successfully demonstrated reversible spatiotemporal presentation of bioactive peptides, as well as patterned attachment and detachment of NIH 3T3 fibroblasts on the surface of these hydrogels. Building on this work, DeForest and Tirrell proposed a new strategy in which the presentation of full-length proteins could be reversibly patterned within a 3D space of PEG hydrogel by combining three bioorthogonal chemistries.³² Specifically, they utilized SPAAC for gel formation, a photomediated oxime

ligation for protein immobilization, and *o*NB photocission for protein removal. Introduction and subsequent removal of biochemical cues in a spatially defined manner were first demonstrated with aldehyde-functionalized proteins. Not only were specific regions of protein introduction achieved, but concentration gradients could also be produced based on a dose-dependent response to light irradiation. Furthermore, since the chemistries used for protein tethering and excision can be initiated using the same light source, intricate patterns comprised of multiple proteins can be created in 3D space. Interestingly, reversible presentation of vitronectin protein within hMSC-laden gels yielded dynamic presentation of osteogenic markers in a spatially controlled manner (Figure 13.4D).

Although these methods have enabled hydrogel modification using small peptides and stable proteins, it is not easy to modify fragile proteins with biological activity reversibly and in a user-defined manner, owing to the random nature in which proteins are conventionally modified (*e.g.* NHS-type chemistry). Toward this, the DeForest group recently demonstrated a modular and robust semisynthetic approach to reversibly pattern cell-laden hydrogels with site-specifically modified proteins.⁸¹ The authors utilized a technique called sortase-tag enhanced protein ligation (STEPL) to design singly modified proteins with bioorthogonal reactive units for PEG hydrogel functionalization. STEPL was utilized to create photopatternable fluorescence proteins, model enzymes, and growth factors that each retain native bioactivity, far outperforming proteins modified using conventional NHS chemistry.^{81,82} These proteins were patterned by mask-based and multiphoton-based laser-scanning lithographic strategies within PEG hydrogels (Figure 13.4E). Human epidermal A431 cells were encapsulated into the PEG hydrogel modified with a photoreleasable green fluorescent protein-epidermal growth factor fusion (EGFP-EGF-*o*NB-N₃). Since canonical EGF signaling requires protein internalization,⁸³ this behavior could be “turned on” with EGF’s photochemical transition from a tethered growth factor to a locally solubilized one. Shadish *et al.* demonstrated the ability to

Figure 13.4 Engineered 3D hydrogel platforms with spatiotemporally programmable biochemical cues: (A) Cytocompatible and spatiotemporal biochemical patterning of 3D hydrogels. Adapted from ref. 22 with permission from Springer Nature, Copyright 2009. (B) Spatiotemporally directed 3D cell motility based on photolytic degradation and biochemical patterning. Adapted from ref. 73 with permission from Springer Nature, Copyright 2011. (C) Selective attachment and detachment of cells through photoreversible presentation of cell-adhesive peptides. Adapted from ref. 80 with permission from John Wiley and Sons, Copyright © 2012 WILEY-VCH Verlag GmbH & Co. KGaA, Weinheim. (D) Spatiotemporal control of hMSC differentiation by photoreversible biochemical patterning with full-length proteins. Adapted from ref. 32 with permission from Springer Nature, Copyright 2015. (E) Spatiotemporal modulation of epidermal intracellular signaling with a photoreleasable growth factors. Adapted from ref. 81 with permission from Springer Nature, Copyright 2019.

confine EGF receptor internalization and canonical activation to one side of a single encapsulate cell. This developed technology is generalizable and can be extended to hydrogels made of natural polymers such as collagen I and fibrin.⁵⁵ These results demonstrate that photochemical control over gel biochemistry can govern 3D biological fate with single-cell and/or sub-cellular resolution, offering exciting routes toward better understanding of how cells respond to transient extracellular biochemical cues.

13.4.3 Adaptable Engineered 3D Matrices for Mechanobiology

In general, some degree of biodegradability is required for cells to migrate through and proliferate within engineered hydrogels. The degradation strategies described in Section 13.4.1 result in an irreversible elimination of the polymer network and potentially undesired release of any immobilized biochemical cues over time. Addressing these limitations, while still allowing for cells to take on *in vivo*-like phenotypes through active matrix remodeling, has given rise to the concept of “adaptable hydrogels” – those crosslinked with reversible bonds that can be broken and reformed without changes in the external environment. Since 2D mechanobiology using adaptable hydrogels and interfaces have already been introduced in Chapters 6 and 11, we will highlight here the importance of an adaptable nature in hydrogel-based 3D culture environments.

In addition to stiffness, matrix viscoelasticity and stress-relaxation have proven important biophysical parameters in the mechanobiological regulation of cell fate (Figure 13.5A).⁸⁴ Formation of cell-laden hydrogels using equilibrium reactions of different strengths (*e.g.* guest–host chemistries,⁸⁵ hydrophobic interactions,⁸⁶ hydrogen bonding,⁸⁷ dynamic covalent linkage⁸⁸) enables creation of hydrogels with tunable viscoelasticity. By comparing cell function in materials that are fully elastic with those that exhibit different degrees of stress relaxation, Chaudhuri and Mooney have demonstrated the substantial impact that stress relaxation has on 2D and 3D cell fate.^{89,90} hMSCs cultured in ionically crosslinked alginate gels with different molecular weighted alginate and PEGylated alginate exhibited different levels of stress relaxation ($t_{1/2} = \sim 1$ h to ~ 1 min). Although the hMSCs encapsulated within nondegradable elastic hydrogel and alginate hydrogel with slower stress relaxation exhibited rounded cell morphologies, increasing the stress relaxation of alginate hydrogels enhanced spreading, proliferation, and osteogenic differentiation and maturation. The proposed mechanism is shown in Figure 13.5B. First, hMSCs within a 3D matrix exert strain on the matrix, resulting in forces/stresses resisting the strain, as determined by the initial elastic modulus of the matrix. In the case of an elastic (nondissipative) matrix, these forces are never relaxed, ultimately yielding no matrix remodeling. In viscoelastic matrixes, however, the forces exerted by cells in the matrix can be relaxed over time because of mechanical yielding and remodeling of the matrix, whereby the rate of matrix stress relaxation

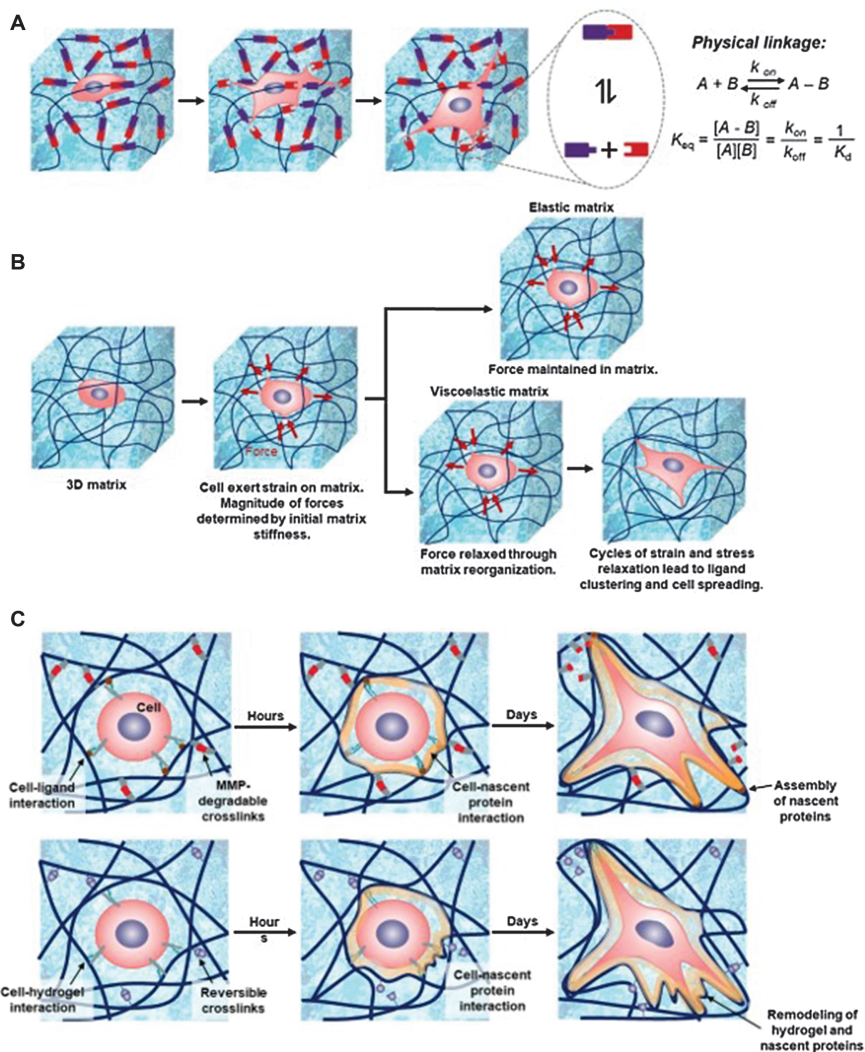


Figure 13.5 Engineered 3D reversibly crosslinked, adaptable hydrogel platforms: (A) Schematic of a conventional adaptable hydrogel incorporating reversible crosslinks. Reproduced from ref. 84 with permission from John Wiley & Sons, Copyright © 2015 WILEY-VCH Verlag GmbH & Co. KGaA, Weinheim. (B) Initial matrix stiffness and stress relaxability regulate MSC state in 3D hydrogels. Reproduced from ref. 89 with permission from Springer Nature, Copyright 2016. (C) Nascent protein adhesion and remodeling govern MSC spreading and fate in both degradable and adaptable hydrogels. Reproduced from ref. 92 with permission from Springer Nature, Copyright 2019.

determines the degree of mechanical remodeling. Similar effects have been observed in other adaptable hydrogels, including PEG-based materials covalently crosslinked through dynamic covalent hydrazone bonds.⁹¹

As discussed here, matrix degradation and remodeling play an important role in regulating the cell behaviors in 3D culture. Loebel *et al.* also demonstrated the impact of early protein deposition on cell behaviors within hydrogel matrices (Figure 13.5C).⁹² Using bioorthogonal noncanonical amino acid tagging that replaces naturally occurring methionine residues in proteins with azidohomoalanine,⁹³ they visualized nascent proteins, which were secreted from hMSCs encapsulated in proteolytically degradable crosslinked hyaluronic acid (HA) hydrogel and viscoelastic physically crosslinked HA hydrogels based on host (cyclodextrin)–guest (adamantane) interactions, within a day of culture. Importantly, the thickness of protein deposit was influenced by hydrogel stiffness, suggesting the ability of the hydrogel to limit cell spreading influences on regulating deposition. They found that nascent protein deposition and remodeling were needed for mechanosensing (YAP/TAZ nuclear translocation) and osteogenic differentiation. Since the native ECM also exhibits some degree of stress relaxation, synthetic culture matrices of a viscoelastic or degradable nature that isolate these effects are of prime interest.

13.4.4 Conclusions and Future Perspective

In native tissue, a variety of biophysicals and biochemicals act synergistically in a complex and coordinated manner to govern cell function and fate. In this chapter, we discussed emerging trends in biomaterial design that afford user-defined programmability of network physiochemistry. At a minimum, biomaterials should enable direct cell encapsulation using methods that are bioorthogonal and cytocompatible. Desirable properties include the ability to mechanically and chemically tune bulk biomaterial properties at the time of encapsulation. Ideal material strategies further offer the ability to modulate biomaterial properties with spatiotemporal control, in an independent and reversible manner, and in the presence of live cells. Though some such systems have been developed and have been used for advanced cell and organoid culture, tremendous opportunities persist in the creation of biomaterial systems that further recapitulate *in vivo* complexity *in vitro*.

In addition to novel biomaterials, so too are new methods needed to better probe 4D cell behavior within these systems. From a mechanobiological perspective, high-throughput techniques that provide real-time information about the local gel microenvironment and how it changes through cell-based matrix remodeling remain in great need. Nondestructive methods to visualize and quantify traction forces exerted by cells on their surrounding matrices also remain of interest, particularly for those that could perform concurrently with user-triggered material alterations. As the ability to regulate cell function spatially continues to evolve, methods that provide single-cell information about cell state but with spatial control would also be tremendously powerful. When coupled with 4D-tunable biomaterials, these strategies are likely to yield many more landmark discoveries in mechanobiology and beyond.

Acknowledgements

This work was supported by a CAREER Award (DMR 1652141, C.A.D.) and a grant (DMR 1807398, C.A.D.) from the National Science Foundation, as well as a Maximizing Investigators' Research Award (R35GM138036, C.A.D.) from the National Institutes of Health. It is also supported in part by AMED-PRIME (JP19gm5810017, K.U.) from the Japan Agency for Medical Research and Development and Grant-in-Aid for Transformative Research Areas (A) (JP20329906, K.U.) from the Japan Society for Promotion of Science.

References

1. N. Wang, J. Butler and D. Ingber, *Science*, 1993, **260**(5111), 1124–1127.
2. A. J. Engler, S. Sen, H. L. Sweeney and D. E. Discher, *Cell*, 2006, **126**(4), 677–689.
3. B. M. Baker and C. S. Chen, *J. Cell Sci.*, 2012, **125**(13), 3015–3024.
4. J. A. Pedersen and M. A. Swartz, *Ann. Biomed. Eng.*, 2005, **33**(11), 1469–1490.
5. S. R. Caliari and J. A. Burdick, *Nat. Methods*, 2016, **13**(5), 405–414.
6. N. Huebsch, P. R. Arany, A. S. Mao, D. Shvartsman, O. A. Ali and S. A. Bencherif, *et al.*, *Nat. Mater.*, 2010, **9**(6), 518–526.
7. J. Zonderland and L. Moroni, *Biomaterials*, 2021, **268**, 120572.
8. P. M. Kharkar, K. L. Kiick and A. M. Kloxin, *Chem. Soc. Rev.*, 2013, **42**(17), 7335–7372.
9. R. C. Bretherton and C. A. DeForest, *ACS Biomater. Sci. Eng.*, 2021, **7**(9), 3997–4008.
10. A. D. Rouillard, C. M. Berglund, J. Y. Lee, W. J. Polacheck, Y. Tsui and L. J. Bonassar, *et al.*, *Tissue Eng., Part C*, 2010, **17**(2), 173–179.
11. J. A. Burdick, A. J. Peterson and K. S. Anseth, *Biomaterials*, 2001, **22**(13), 1779–1786.
12. S. J. Bryant and K. S. Anseth, *J. Biomed. Mater. Res.*, 2002, **59**(1), 63–72.
13. S. J. Bryant and K. S. Anseth, *J. Biomed. Mater. Res., Part A*, 2003, **64A**(1), 70–79.
14. E. R. Ruskowitz and C. A. DeForest, *ACS Biomater. Sci. Eng.*, 2019, **5**(5), 2111–2116.
15. A. M. Kloxin, C. J. Kloxin, C. N. Bowman and K. S. Anseth, *Adv. Mater.*, 2010, **22**(31), 3484–3494.
16. C. M. Madl and S. C. Heilshorn, *Adv. Funct. Mater.*, 2018, **28**(11), 1706046.
17. D. A. Ossipov and J. Hilborn, *Macromolecules*, 2006, **39**(5), 1709–1718.
18. A. M. Testera, A. Girotti, I. G. de Torre, L. Quintanilla, M. Santos and M. Alonso, *et al.*, *J. Mater. Sci.: Mater. Med.*, 2015, **26**(2), 105.
19. V. Hong, N. F. Steinmetz, M. Manchester and M. G. Finn, *Bioconjugate Chem.*, 2010, **21**(10), 1912–1916.
20. J. M. Baskin, J. A. Prescher, S. T. Laughlin, N. J. Agard, P. V. Chang and I. A. Miller, *et al.*, *Proc. Natl. Acad. Sci. U. S. A.*, 2007, **104**(43), 16793–16797.

21. J. A. Codelli, J. M. Baskin, N. J. Agard and C. R. Bertozzi, *J. Am. Chem. Soc.*, 2008, **130**(34), 11486–11493.
22. C. A. DeForest, B. D. Polizzotti and K. S. Anseth, *Nat. Mater.*, 2009, **8**(8), 659–664.
23. C. A. DeForest, E. A. Sims and K. S. Anseth, *Chem. Mater.*, 2010, **22**(16), 4783–4790.
24. E. A. Sims, C. A. DeForest and K. S. Anseth, *Tetrahedron Lett.*, 2011, **52**(16), 1871–1873.
25. J. C. Jewett, E. M. Sletten and C. R. Bertozzi, *J. Am. Chem. Soc.*, 2010, **132**(11), 3688–3690.
26. M. F. Debets, S. S. van Berkel, S. Schoffelen, F. P. J. T. Rutjes, J. C. M. van Hest and F. L. van Delft, *Chem. Commun.*, 2010, **46**(1), 97–99.
27. A. Kuzmin, A. Poloukhtine, M. A. Wolfert and V. V. Popik, *Bioconjugate Chem.*, 2010, **21**(11), 2076–2085.
28. C. D. Hermann, D. S. Wilson, K. A. Lawrence, X. Ning, R. Olivares-Navarrete and J. K. Williams, *et al.*, *Biomaterials*, 2014, **35**(36), 9698–9708.
29. J. Zheng, L. A. Smith Callahan, J. Hao, K. Guo, C. Wesdemiotis and R. A. Weiss, *et al.*, *ACS Macro Lett.*, 2012, **1**(8), 1071–1073.
30. X. Wang, Z. Li, T. Shi, P. Zhao, K. An and C. Lin, *et al.*, *Mater. Sci. Eng. C*, 2017, **73**, 21–30.
31. J. Dommerholt, S. Schmidt, R. Temming, L. J. A. Hendriks, F. P. J. T. Rutjes and J. C. M. van Hest, *et al.*, *Angew. Chem., Int. Ed.*, 2010, **49**(49), 9422–9425.
32. C. A. DeForest and D. A. Tirrell, *Nat. Mater.*, 2015, **14**(5), 523–531.
33. C. M. Madl, L. M. Katz and S. C. Heilshorn, *Adv. Funct. Mater.*, 2016, **26**(21), 3612–3620.
34. R. van Geel, G. J. M. Pruijn, F. L. van Delft and W. C. Boelens, *Bioconjugate Chem.*, 2012, **23**(3), 392–398.
35. Z. Li, T. S. Seo and J. Ju, *Tetrahedron Lett.*, 2004, **45**(15), 3143–3146.
36. V. X. Truong, M. P. Ablett, H. T. J. Gilbert, J. Bowen, S. M. Richardson and J. A. Hoyland, *et al.*, *Biomater. Sci.*, 2014, **2**(2), 167–175.
37. H.-L. Wei, Z. Yang, L.-M. Zheng and Y.-M. Shen, *Polymer*, 2009, **50**(13), 2836–2840.
38. C. M. Nimmo, S. C. Owen and M. S. Shoichet, *Biomacromolecules*, 2011, **12**(3), 824–830.
39. S. Kirchhof, F. P. Brandl, N. Hammer and A. M. Goepferich, *J. Mater. Chem. B*, 2013, **1**(37), 4855–4864.
40. M. L. Blackman, M. Royzen and J. M. Fox, *J. Am. Chem. Soc.*, 2008, **130**(41), 13518–13519.
41. H. Zhou, J. Woo, A. M. Cok, M. Wang, B. D. Olsen and J. A. Johnson, *Proc. Natl. Acad. Sci.*, 2012, **109**(47), 19119–19124.
42. D. L. Alge, M. A. Azagarsamy, D. F. Donohue and K. S. Anseth, *Biomacromolecules*, 2013, **14**(4), 949–953.
43. A. Gress, A. Völkel and H. Schlaad, *Macromolecules*, 2007, **40**(22), 7928–7933.

44. A. E. Rydholm, C. N. Bowman and K. S. Anseth, *Biomaterials*, 2005, **26**(22), 4495–4506.
45. C. N. Salinas, B. B. Cole, A. M. Kasko and K. S. Anseth, *Tissue Eng.*, 2007, **13**(5), 1025–1034.
46. M. P. Lutolf, J. L. Lauer-Fields, H. G. Schmoekel, A. T. Metters, F. E. Weber and G. B. Fields, *et al.*, *Proc. Natl. Acad. Sci.*, 2003, **100**(9), 5413–5418.
47. M. P. Lutolf, N. Tirelli, S. Cerritelli, L. Cavalli and J. A. Hubbell, *Bioconjugate Chem.*, 2001, **12**(6), 1051–1056.
48. M. P. Lutolf, G. P. Raeber, A. H. Zisch, N. Tirelli and J. A. Hubbell, *Adv. Mater.*, 2003, **15**(11), 888–892.
49. E. A. Phelps, N. O. Enemchukwu, V. F. Fiore, J. C. Sy, N. Murthy and T. A. Sulchek, *et al.*, *Adv. Mater.*, 2012, **24**(1), 64–70.
50. A. Shikanov, R. M. Smith, M. Xu, T. K. Woodruff and L. D. Shea, *Biomaterials*, 2011, **32**(10), 2524–2531.
51. M. Malkoch, R. Vestberg, N. Gupta, L. Mespouille, P. Dubois and A. F. Mason, *et al.*, *Chem. Commun.*, 2006, **26**, 2774–2776.
52. B. D. Fairbanks, M. P. Schwartz, A. E. Halevi, C. R. Nuttelman, C. N. Bowman and K. S. Anseth, *Adv. Mater.*, 2009, **21**(48), 5005–5010.
53. G. N. Grover, J. Lam, T. H. Nguyen, T. Segura and H. D. Maynard, *Biomacromolecules*, 2012, **13**(10), 3013–3017.
54. P. E. Farahani, S. M. Adelmund, J. A. Shadish and C. A. DeForest, *J. Mater. Chem. B*, 2017, **5**(23), 4435–4442.
55. I. Batalov, K. R. Stevens and C. A. DeForest, *Proc. Natl. Acad. Sci.*, 2021, **118**(4), e2014194118.
56. E. Saxon and C. R. Bertozzi, *Science*, 2000, **287**(5460), 2007–2010.
57. K. M. Gattás-Asfura, C. A. Fraker and C. L. Stabler, *J. Biomed. Mater. Res., Part A*, 2011, **99A**(1), 47–57.
58. S. Khetan, M. Guvendiren, W. R. Legant, D. M. Cohen, C. S. Chen and J. A. Burdick, *Nat. Mater.*, 2013, **12**(5), 458–465.
59. T. Sato and H. Clevers, *Science*, 2013, **340**(6137), 1190–1194.
60. J. Kim, B.-K. Koo and J. A. Knoblich, *Nat. Rev. Mol. Cell Biol.*, 2020, **21**(10), 571–584.
61. R. Cruz-Acuña, M. Quirós, A. E. Farkas, P. H. Dedhia, S. Huang and D. Siuda, *et al.*, *Nat. Cell Biol.*, 2017, **19**, 1326.
62. N. O. Enemchukwu, R. Cruz-Acuña, T. Bongiorno, C. T. Johnson, J. R. García and T. Sulchek, *et al.*, *J. Cell Biol.*, 2015, **212**(1), 113–124.
63. M. A. Rice and K. S. Anseth, *J. Biomed. Mater. Res., Part A*, 2004, **70A**(4), 560–568.
64. S. J. Bryant, R. J. Bender, K. L. Durand and K. S. Anseth, *Biotechnol. Bioeng.*, 2004, **86**(7), 747–755.
65. N. Gjorevski, N. Sachs, A. Manfrin, S. Giger, M. E. Bragina and P. Ordóñez-Morán, *et al.*, *Nature*, 2016, **539**(7630), 560–564.
66. M. J. Wilson, S. J. Liliensiek, C. J. Murphy, W. L. Murphy and P. F. Nealey, *Soft Matter*, 2012, **8**(2), 390–398.
67. G. Maheshwari, G. Brown, D. A. Lauffenburger, A. Wells and L. G. Griffith, *J. Cell Sci.*, 2000, **113**(10), 1677–1686.

68. B. Trappmann, J. E. Gautrot, J. T. Connelly, D. G. T. Strange, Y. Li and M. L. Oyen, *et al.*, *Nat. Mater.*, 2012, **11**(7), 642–649.
69. V. Hernandez-Gordillo, T. Kassis, A. Lampejo, G. Choi, M. E. Gamboa and J. S. Gnecco, *et al.*, *bioRxiv*, 2019, 806919.
70. E. R. Ruskowitz and C. A. DeForest, *Nat. Rev. Mater.*, 2018, **3**, 17087.
71. A. M. Kloxin, A. M. Kasko, C. N. Salinas and K. S. Anseth, *Science*, 2009, **324**(5923), 59–63.
72. A. M. Kloxin, M. W. Tibbitt and K. S. Anseth, *Nat. Protoc.*, 2010, **5**(12), 1867–1887.
73. C. A. DeForest and K. S. Anseth, *Nat. Chem.*, 2011, **3**(12), 925–931.
74. D. R. Griffin and A. M. Kasko, *J. Am. Chem. Soc.*, 2012, **134**(31), 13103–13107.
75. T. E. Brown, I. A. Marozas and K. S. Anseth, *Adv. Mater.*, 2017, **29**(11), 1605001.
76. T. F. Scott, A. D. Schneider, W. D. Cook and C. N. Bowman, *Science*, 2005, **308**(5728), 1615–1617.
77. R. G. Wylie, S. Ahsan, Y. Aizawa, K. L. Maxwell, C. M. Morshead and M. S. Shoichet, *Nat. Mater.*, 2011, **10**(10), 799–806.
78. Y. Aizawa, R. Wylie and M. Shoichet, *Adv. Mater.*, 2010, **22**(43), 4831–4835.
79. N. Broguiere, I. Luchtefeld, L. Trachsel, D. Mazunin, R. Rizzo and J. W. Bode, *et al.*, *Adv. Mater.*, 2020, **32**(25), e1908299.
80. C. A. DeForest and K. S. Anseth, *Angew. Chem., Int. Ed.*, 2012, **51**(8), 1816–1819.
81. J. A. Shadish, G. M. Benuska and C. A. DeForest, *Nat. Mater.*, 2019, **18**(9), 1005–1014.
82. P. M. Gawade, J. A. Shadish, B. A. Badeau and C. A. DeForest, *Adv. Mater.*, 2019, **31**(33), 1902462.
83. P. R. Kuhl and L. G. Griffith-Cima, *Nat. Med.*, 1996, **2**(9), 1022–1027.
84. H. Wang and S. C. Heilshorn, *Adv. Mater.*, 2015, **27**(25), 3717–3736.
85. C. B. Rodell, A. L. Kaminski and J. A. Burdick, *Biomacromolecules*, 2013, **14**(11), 4125–4134.
86. Y. Liu, B. Liu, J. J. Riesberg and W. Shen, *Macromol. Biosci.*, 2011, **11**(10), 1325–1330.
87. H. Tan, C. Xiao, J. Sun, D. Xiong and X. Hu, *Chem. Commun.*, 2012, **48**(83), 10289–10291.
88. B. Yang, Y. Zhang, X. Zhang, L. Tao, S. Li and Y. Wei, *Polym. Chem.*, 2012, **3**(12), 3235–3238.
89. O. Chaudhuri, L. Gu, D. Klumpers, M. Darnell, S. A. Bencherif and J. C. Weaver, *et al.*, *Nat. Mater.*, 2016, **15**(3), 326–334.
90. O. Chaudhuri, L. Gu, M. Darnell, D. Klumpers, S. A. Bencherif and J. C. Weaver, *et al.*, *Nat. Commun.*, 2015, **6**, 6365.
91. D. D. McKinnon, D. W. Domaille, J. N. Cha and K. S. Anseth, *Adv. Mater.*, 2014, **26**(6), 865–872.
92. C. Loebel, R. L. Mauck and J. A. Burdick, *Nat. Mater.*, 2019, **18**(8), 883–891.
93. D. C. Dieterich, J. J. Lee, A. J. Link, J. Graumann, D. A. Tirrell and E. M. Schuman, *Nat. Protoc.*, 2007, **2**(3), 532–540.